Analytical Methods

Accepted Manuscript

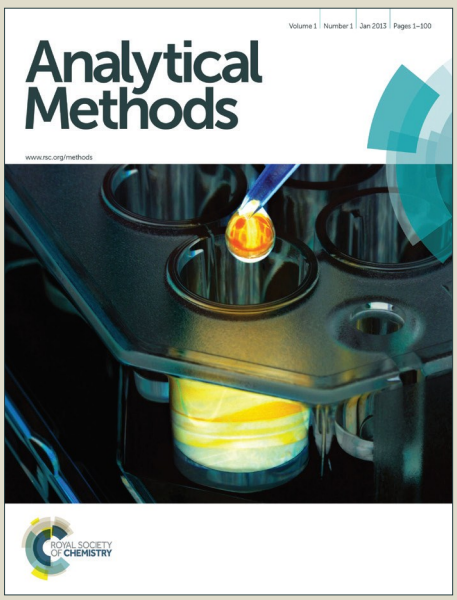

This is an *Accepted Manuscript*, which has been through the Royal Society of Chemistry peer review process and has been accepted for publication.

Accepted Manuscripts are published online shortly after acceptance, before technical editing, formatting and proof reading. Using this free service, authors can make their results available to the community, in citable form, before we publish the edited article. We will replace this *Accepted Manuscript* with the edited and formatted *Advance Article* as soon as it is available.

You can find more information about *Accepted Manuscripts* in the Information for Authors.

Please note that technical editing may introduce minor changes to the text and/or graphics, which may alter content. The journal's standard Terms & Conditions and the Ethical guidelines still apply. In no event shall the Royal Society of Chemistry be held responsible for any errors or omissions in this *Accepted Manuscript* or any consequences arising from the use of any information it contains.

ROYAL SOCIETY OF CHEMISTRY

www.rsc.org/methods

A biopolymeric nano-receptor for sensitive and selective recognition of albendazole

Juhi Srivastava and Meenakshi Singh*
Department of Chemistry, MMV
Banaras Hindu University, Varanasi-221005, INDIA
E-mail: meenakshi@bhu.ac.in, meenakshibhu70@gmail.com

Abstract

A molecularly imprinted electrochemical sensor was developed for albendazole (ABZ) based on chitosan nanoparticles. The polymeric film was formed on the surface of gold electrode by electrodepositing nanoparticles of biopolymer chitosan in presence of ABZ template by cyclic voltammetry (CV). Various parameters were optimized for controlling the performance of molecularly imprinted polymer (MIP) modified sensor. The prepared MIP sensor was specific towards ABZ and the recognition was analyzed by differential pulse voltammetry (DPV) to verify the changes in currents. In the optimal condition, response of MIP sensor to ABZ was linearly proportional to its concentration with limit of detection (LOD) as 0.119 μg mL^{-1}. Hence, a sensitive and selective electrochemical sensor in ecofriendly biopolymer-derived nanoconfiguration for ABZ has been reported here *via* imprinting approach.

Keywords: Chitosan, nanoparticles, molecular imprinting, albendazole, electrodeposition, Differential pulse voltammetry

Introduction

Chitosan nanoparticles offer many advantages to be incorporated in various tools and technologies being developed by sensing fraternity. Chitosan is a suitable biopolymer as this natural polymer has excellent properties such as biocompatibility, biodegradability, non-toxicity and adsorption properties. Chitosan being environment friendly with such excellent characteristics prompted us to exploit it as polymeric format for developing molecularly imprinted polymers (MIP). Chitosan nanoparticles with selective molecular recognition properties are attractive as they can easily be incorporated into existing analytical or preparative platforms to unravel various practical problems. An attempt is made here to use biopolymer chitosan as a polymeric format to imprint the drug, albendazole (ABZ) in nano-configuration. Molecular imprinting offers creation of artificial receptor in a facile manner [1]. MIPs often named as 'artificial enzymes' and/or 'artificial antibodies' are one of the most promising technique in sensor designing. The major benefits of MIPs compared with antibodies are their high and almost unlimited-stability and easy way of preparation at a large scale that unquestionably outperform antibodies in terms of costs.

ABZ chemically known as methyl [5-propolythio-1H-benzimidazol-2-yl] carbamate is a member of benzimidazole compounds which are widely used as antihelminthic drug against parenchymal brain neurocysticercosis, an infection of central nervous system caused by larva of *Taenia solium* [2-4] and various other parasitic worm infections. ABZ enzymatically metabolizes to albendazole sulphoxide (ASOX) initially and subsequently to albendazole sulphone (ASON) [5-7] in gastrointestinal tract. Overusage of pharmaceutical drugs and their disposal is matter of concern as their accumulation as such or their metabolites in various environmental segments harm the global healthcare. A quantitative analytical method for the determination of ABZ is

warranted for its monitoring and optimization of clinical therapy in patients. Several methods have been proposed for the determination of ABZ or its metabolites, for instance by voltammetric detection at glassy carbon electrode (linear sweep (LSV), square wave (SWV) and differential pulse voltammetry (DPV))[8], differential pulse cathodic stripping voltammetry (DPCSV) at hanging drop mercury electrode (HMDE)[9], SWV at modified glassy carbon rotating electrode[10], LSV at glassy carbon rotating disc electrode[11], DPV at boron doped diamond electrode[12], liquid chromatography[13], liquid chromatography using fluorescence detection [14,15], HPLC[16-18], spectrophotometry by using chloramine-T[19], UV spectrophotometry [20], visible spectrophotometry[21], gas chromatography - mass spectrometry [22], differential scanning calorimetry (DSC) with HPLC[23-25], colorimetry[26], and fluorometric analysis [27]. Another benzimidazole drug, mebendazole was estimated by cathodic stripping voltammetry (CSV) at graphene-chitosan composite modified glassy carbon electrode[28]. Although ABZ has been estimated by various analytical methods earlier as reported above, but only one group has attempted to use molecular imprinting for its estimation in organic media *via* bulk imprinting[29]. A restraint in bulk imprinting is high crosslinking nature of MIPs which limits the extraction of the original templates located at interior area of the bulk materials which results in incomplete template removal, small binding capacity and slow mass transfer. Surface imprinting largely circumvents these limitations, as the imprinted templates are situated at the surface or in the proximity of the material's surface. Novelty of work lies in the detection of ABZ by a simple, facile, cost-effective, sensitive and selective but still easy to fabricate sensor by molecular imprinting of biopolymer chitosan in nanoformat.

2. Materials and Methods

2.1 Materials

Chitosan (medium molecular weight) and ABZ is purchased from Sigma-Aldrich. Tripolyphosphate (TPP) was procured from Molychem while glutaraldehyde from Spectrochem, acetic acid from Merck Specialities Pvt. Ltd., disodium hydrogen orthophosphate (anhydrous) and sodium dihydrogen orthophosphate (dehydrate) were purchased from Fischer Scientific. Human blood plasma samples were collected from Institute of Medical Science (IMS), Banaras Hindu University (BHU) (Varanasi, India) as per approved protocol by the institutional ethical committee of the IMS, BHU after patients' written informed consent.

2.2 Instruments

All electrochemical measurements were performed on a CHI 410B electrochemical workstation with three electrode system (a gold electrode, a platinum wire and Ag/AgCl electrode were used as working, counter and reference electrodes respectively). A magnetic stirrer (Ika model-C-MAG HS7) was employed to stir test solutions during measurements. A homemade gold electrode with exposed surface area of 0.39 cm^2 was used as a working electrode. Prior to use, surface of the gold electrode was polished carefully and then sonicated in ethanol and deionized water for 10 min, respectively. In order to remove trace alumina and other possible contamination on surface of gold electrode, the polished electrode was subjected to cyclic potential sweeping between 0 and 1.5 V in 0.5 mol/L sulfuric acid until a stable cyclic voltammogram was obtained. The infrared spectra were recorded using Jasco FTIR 5300 from 400 to 4000 cm^{-1}. Atomic force microscopy (AFM) was performed by instrument Solver Next model of NT-MDT Company which is used for visualization of evaluation of surface dominant

feature. Contact mode with soft silicon nitride tip, covered with reflective gold coating on the back side, was used in order to obtain the topography images. The AFM imaging was performed in air. The scanned area of the sample 5nm x 5nm and scan rate of AFM was 0.5Hz.

2.3 Synthesis of Chitosan Nanoparticles

Chitosan nanoparticle was prepared by using ionotropic gelation method [30-32]. The mechanism of chitosan nanoparticle formation is based on electrostatic interaction between amine group of chitosan and negative charge of polyanion tripolyphosphate (TPP) [33]. This technique offers a simple and mild preparation method in the aqueous environment. Chitosan solution (0.075 g. 25 mL^{-1}) was prepared in aqueous solution of acetic acid (1 %) under constant stirring over magnetic stirrer at 60^{o}C for 5h. pH of resulting chitosan solution was adjusted to 5.5 with 0.1 M NaOH. Under magnetic stirring at room temperature, 10 ml of 1% (w/v) aqueous solution of TPP was added dropwise using syringe (0.3 mL min^{-1}). The stirring was continued for 2 h more.

2.4 Preparation of Molecularly imprinted polymer (MIP)

The MIP was prepared by electrodepositing chitosan nanoparticles with analyte molecules (ABZ) on the surface of the gold electrode. Chitosan nanoparticles (50 mg) were suspended in 10% acetic acid solution by heating with stirring at 60^{0}C for 5 h (25 mL solution). A solution of ABZ was separately prepared (0.01 g ABZ in 12.5 mL of 20% acetic acid) by stirring at room temperature for 30 min. Subsequently, ABZ solution was added to the nanoparticle solution and solution was stirred at room temperature for 2 h followed by addition of glutaraldehyde solution (2.5 mL) as cross-linking agent (0.5 mL in 2 mL water) with constant stirring at room temperature for 15 min. This solution was electrodeposited with supporting electrolyte (phosphate buffer solution, pH 7 in a 2:1 (*v/v*) ratio) using cyclic voltammetry (CV).

Electrodeposition was completed in 30 cycles. Non-imprinted polymer (NIP) was also prepared in similar manner without the template (ABZ) in electrodeposition solution. ABZ molecules were extracted with a solution of acetic acid and methanol (1:4, *v*/*v*) on ultrasonicating with heating for 25 min (Fig. 1). The extracted solution was verified by differential pulse voltammetry (DPV) for extraction of the template molecule at glassy carbon electrode. The schematic representation of imprinting and removal of ABZ from imprinted polymer-modified gold electrode is shown in Fig. 2.

3. Result & Discussion

3.1 Electrodeposition and characterization of MIP and NIP films

FTIR spectra of chitosan nanopaticles is shown in Fig. 3 which differs from spectra of chitosan (bulk) cited in literature[34,35]. The absorptions at 3412 cm^{-1} is attributed to hydrogen bonded O-H st which becomes wider in nanoparticles. The peaks of N-H stretching from amine and amide are overlapped in the same region (3500-3300 cm^{-1}). The absorptions at 2926 and 2858 is due to C-H st and at 1095 is due to (C-O-C) stretching whereas 1645 cm^{-1} absorption is due to carbonyl stretching of amide which is a little shifted. The absorptions at 1160 cm^{-1} is due to P=O, showing linkage between phosphoric and ammonium ion confirming the interaction between tripolyphosphoric groups with ammonium group of chitosan. The spectrum of chitosan nanoparticle indicates the spectrum of a complex having chitosan and TPP which is seen in region 1700 -1500 cm^{-1} and 890 cm^{-1}. AFM image of chitosan nanoparticles, shown in Fig. 4 evinces the nanosize of particles.

Cyclic voltammogram for electrodeposition of chitosan nanoparticles with and without ABZ is shown in Fig. 5. The thickness of deposition layers increased as the deposition time increased, leading to diminished conductivity of electrode, thus reducing the peak current in

subsequent cycles. In first cycle, chitosan nanoparticles were electrodeposited at anodic potential of 0.547V and the peak current dropped significantly with each scan. Current change is significant in initial cycles attaining a saturated value in 30 cycles on deposition of a stabilized layer of polymeric film on electrode. Another peak current at 1.12 V due to oxidation of ABZ was observed for MIP film (Fig 5a). The electrochemical method has been proposed to identify ABZ based on oxidation of ABZ to ASOX[8,9,] Although two different metabolites ASOX and ASON are produced due to the oxidation of ABZ [5], but the formation of ASON is not verified electrochemically. The observed current is ascribed to oxidation of sulphur atom present in the molecule. Aliphatic or aromatic sulphides are oxidized to their dication form at room temperature (25^0C) in aprotic solvents in a two electron process. These species further participate in dimerization reaction or sulphonium ion formation [36].

$$C_{12}H_{15}N_3O_2S \longrightarrow C_{12}H_{15}N_3O_2S^{2+} + 2e^- \quad (1)$$

DPV have shown that ABZ gives a well defined anodic peak at potential E_p 1.12V.

3.3 Extraction of ABZ from MIP film

MIP film electrodeposited on electrode was first rinsed thoroughly with copious amount of water to remove physisorbed species. The ABZ template was extracted from MIP film with a solution of acetic acid and methanol (1:4 *v/v* ratio). Removal of ABZ was confirmed by DPV (Fig.1). DPV measurements of the solution after extraction of ABZ from MIP film were carried out on glassy carbon electrode. A peak at 1.12 V confirmed the removal of ABZ (Fig. 1).

3.4 Electrochemical responses of MIP, NIP and bare gold electrodes

DPV was used for indirect estimation of ABZ molecules in the MIP film. In this procedure, a $K_3Fe(CN)_6$ redox probe is utilized, Fig. 6 shows the behaviour of this redox probe on NIP film-coated gold electrode (curve a), MIP- film coated gold electrode with ABZ molecules (curve b)

and after extraction of ABZ molecules (curve c). Curve d shows the response of redox probe on bare gold electrode. Curve a shows the response of NIP film coated on electrode which corroborates non-conducting nature of NIP film. In DPV experiment, ABZ molecules occupying imprinted cavities of the MIP film prevented diffusion of this redox probe from bulk solution through film to the electrode surface. After extraction of template from imprinted sites, DPV peak size is enhanced (curve c) depicting the creation of imprinted sites (cavities) facilitating probe molecules to reach on electrode surface. Hence creation of imprinted cavities were proven to be generated on MIP film deposited on electrode, on rebinding of template molecules, these cavities are blocked so hindering probe molecules to reach on electrode surface (Fig. 7). It was difficult for probe molecules to go through the quite compact coating and arrive at the interface to redox due to low conductivity of chitosan polymer. On extraction of ABZ molecules, complementary cavities on surface of electrode are generated which facilitate diffusion of redox probe towards electrode surface. Thus by probing electrochemical activity of the $[Fe(CN)_6]^{3-/4-}$ redox couple at the MIPs-coated electrode using DPV can indirectly determine ABZ (Fig 7). The DPV current response for MIP and NIP for template rebinding is shown in Fig. 8. Fig. 9 shows rebinding at MIP modified gold electrode and rebinding at NIP modified gold electrode. The imprinting effect of MIP is often assessed by imprinting factor (IF). For this ABZ-imprinted polymer coated gold electrode sensor, IF is found to be 2.89, indicating the selectivity of ABZ compared with NIP coated electrode. Such data verifies the fact that this MIP sensor possesses good selectivity for ABZ due to preset recognition sites created during imprinting process which was propounded to be originating from 'stoichiometric noncovalent interactions'.

3.4 Response of MIP towards pH

For effective interaction between ABZ and MIP binding sites, the complementarity between binding sites of imprinted chitosan film and ABZ should remain intact. The effect of pH on the current response was investigated by DPV in pH range of 2.0-10.0 (Fig 10). Lima *et al.* have drawn Pourbaix diagram (E *vs* pH) for ABZ and studied detail mechanistic aspects of its oxidation[37]. DPV current obtained on rebinding of ABZ is lower when pH of rebinding solution of ABZ is acidic (pH 2-4) and increases continuously in pH range 4 to 7. But as the alkalinity is approached, current drops sharply. The oxidation peak potential of ABZ is pH dependent. The peak potential decreases approximately in the studied process which is consistent with an electrochemical mechanism involving $2H^+$ and two electrons[22]. ABZ shows maximum (negative) peak current in the pH region 4 to 7 which roughly falls between pka_1 (2.80) and pka_2 (10.26) of ABZ[38]. Due to low solubility of ABZ in water, rebinding solution of ABZ was prepared in 20% acetic acid rendering ABZ molecules in protonated form $ABZH_2^+$. On increasing the pH of solution between 2.80 and 10.26, molecules will be in ABZH form and beyond pH 10.26, it should exist in ABZ^- form. While the imprinting format also has ionic nature *i.e.* chitosan nanoparticles comprising of ionic centres of tripolyphosphoric groups under interaction with ammonium centres of chitosan. The anodic peak current showed to be increased as pH rises from 4 to 7. However further increase in the pH of rebinding solution decreases slowly the peak height. Hence in corroboration with specific imprints created for ABZH form of template, rebinding is most at pH 7. Therefore phosphate buffer with pH 7 was used as supporting electrolyte in all voltammetric determination.

3.6 Cross-selectivity study

For assessment of selectivity of ABZ MIP film, cross reactivity with respect to functionally and structurally similar interfering agents, such as 5-aminosalicylic acid (5ASA), antipyrine, 3-

thiophene acetic acid (3TAA), l-phenylalanine was compared. The respective plots are shown in Fig 11 illustrating the response of MIP at optimized parameters towards interferents. The highest sensitivity was obtained for ABZ. The template fits into imprinted cavity driven by electrostatic interaction in this study followed by aligning of functional groups on MIP around template molecule's conformational orientation. The selectivity was more prominent at lower concentrations where specific imprints made only for ABZ do not bind effectively the interferrant molecules in comparison to ABZ that just fits and binds in those cavities giving highest sensitivity.The small current response of different analogoues of ABZ could be easily understood that although there were similar structure in terms of size and functional groups, they still mismatched the imprinting sites of ABZ. The MIP sensor was able to detect a large range of ABZ because of the presence of pre-shaped functionalized cavities in MIP backbone. Although, these analogues were different from ABZ in molecular size but they also had some chances of approaching the imprinting sites of MIP backbone. From the DPV experiments, it was easily understood that the electrochemically developed MIP sensor possessed a selective recognition towards ABZ.

3.7 Analytical Applications

In order to evaluate the feasibility of the ABZ-MIP electrochemical sensor for clinical application, it was used to determine ABZ in real samples (blood plasma) according to the proposed method (Fig. 12). As can be seen the matrix components of blood plasma are not affecting the MIP sensor. Fig 13 shows the calibration plot for ABZ-imprinted sensor and Fig 7 shows the current-voltage profile of DPV run on rebinding of template with solutions of varying concentration. Good linear relationship was obtained with $R^2 = 0.9577$. Detection limit for ABZ template in aqueous solution by MIP-sensor is calculated as 0.119 μg mL^{-1} following standard

analytical method[39]. The proposed sensor was also compared with other reported methods for ABZ detection (Table 1). Insofar as the earlier reported methods, to obviate the matrix effect, either pre-treatment or derivatization is often required and moreover they are not economical and robust under ambient conditions[14,19]. The present method is simple, cost-effective, reproducible and can detect the trace level of ABZ.

4. Conclusion

In present work, an attempt is made to use biopolymer chitosan as a polymeric format to imprint the drug ABZ. Electrodeposition of chitosan nanoparticles with template ABZ and crosslinker glutaraldehyde on gold electrode is utilized to imprint ABZ, which was able to detect ABZ at trace level with imprinting factor of 2.89. High sensitivity and improved detection limit are promising for determination of ABZ. The proposed biopolymer-derived electrochemical sensor is effective for the determination of ABZ, being simple, inexpensive, ecofriendly and rapid.

Acknowledgements: Authors acknowledge Department of Chemistry, Banaras Hindu University for AFM analysis and financial support by the Council of Scientific and Industrial Research, New Delhi [No 01(2769)/13/EMR-II].

5. References

1. M.J.Whitecomb, N.Kirsch, I.Nicholls, 2014. *J. Mol. Recognit.* 2014, **27**, 297-401.
2. O.M.Takayanagui, E.Jardim, *Arch. Neurol.* 1992, **49**, 290-294.
3. O.H.Del Brutto, *Arch. Neurol.*1995, **52**, 102-104.
4. O.H.Del Brutto, J.Sotelo, G.C.Roman, *Clin. Infect. Dis.*1993, **17**, 730-735.
5. C.Villaverde, A.I.Alvarez, P.Redondo, J.Voces, J.L.Del Estal, J.G.Prieto, *Xenobiotica*. 1995, **25**, 433-441.
6. M.P.Marques, O.M.Takaynagui, V.L.Lanchote, *Braz. J. Med. Biol. Res*. 2002, **35**, 261-269.
7. J.Sotelo, H.Jung, *Clin. Pharmacokinet*. 1998, **34**, 503-515.
8. M.F.Oliveira, N.R.Stradiotto, *Anal. Lett.* 2001, **34**, 377-387.
9. A.Z.Abu Zuhri, A.I.Hussein, M.Musmar, S.Yaish, *Anal. Lett.* 1999, 32, 15, 2965-2975.

10. T.A.M.Msagati, J.C.Ngila, *S. Afr. J. Chem.* 2003, **56**, 5–9.
11. A.L.Santos, R.M.Takeuchi, M.P.Mariotti, M.F.De Oliveira, M.V.B.Zanoni, N.R.Stradiotto, *Farmaco II*, 2005, *60*, 671–674.
12. B.C.Lourencao, M.Baccarin, R.A.Medeiros, R.C.Rocha-Filho, O.Fatibello-Filho, *J Electroanal Chem.* 2013, **707**, 15–19.
13. A.Waldia, S.Gupta, R.Issarani, B.P.Nagori, *Indian J. Chem. Techn.*, 2008, **15**, 617–620.
14. D.J.Fletouris, N.A.Botsoglou, I.E.Psomas, A.I.Mantis, *Anal. Chim. Acta.* 1997, **345**, 111-119.
15. D.S.Nakos, N.A.Botsoglou, I.E.Psomas, *J. Liquid Chromatogr.* 1994, **17**, 4145-4155.
16. M.Hurtado, M.T.Medina, J.Sotelo, H.Jung, *J Chromatogr.* 1989, **494**, 403-407.
17. D.Kitzman, K.J.Cheng, L.Fleckenstein, *J. Pharm Biomed Anal.* 2002, **30**, 801-813.
18. R.Sarin, A.P.Dash, A.K.Dua, *J. Chromatogr B*, 2004, **799**, 233-238.
19. K.Basavaiah, H.C.Prameela, *Il Farmaco*. 2003, **58**, 527-534.
20. S.C.Mandal, M.Bhattacharyya, A.K.Maity, B.K.Guptha, S.K.Ghosal, *Indian Drugs*, 1992, **29**, 323-324.
21. C.S.P.Sastry, V.A.N.Sarma, U.V.Prasad, C.S.R.Lakshmi, *Indian J. Pharm. Sci.* 1997, **59**, 161-164.
22. R.G.Lima, P.S.Bonato, R.S.Silva, *J.Pharma Biomed Anal.* 2003, **32**, 337-343.
23. C.E.P.Malan, A.D.De-Villiers, M.M.Loetter, *Drug Dev. Ind. Pharm.* 1997, **23**, 533-537.
24. W.J.Blanchflower, A.Cannavan, D.G.Kennedy, *Analyst* 1994, **119**, 1325–1328.
25. J.A.Bogan, S.Marriner, *J. Pharm. Sci.* 1980, **69**, 422–423.
26. N.C.Sangster, R.K.Prichard, E.Lacey, *J. Parasit.* 1985, 645–651.
27. W.R.Baeyens, F.A.Fattah, P.D.Moerloose, *Anal. Lett.* 1985, **18**, 2143–2154.
28. M.Ghalkhania, S.Shahrokhian, *Sensor Actuat B-Chem.* 2013, **185**, 669-674.
29. C.Cacho, E.Turiel, C.Perez-Conde, *Talanta* 2009, **78**, 1029-1035.
30. P.Calvo, C.Remunan-Lopez, J.L.Vila-Jato, M.J.Alonso, *J. Appl. Polym. Sci.* 1997, **63**, 125-132.
31. K.A.Janes, M.P.Fresneau, A.Marazuela, A.Fabra, M.J.Alonso, *J. Control. Release*. 2001, **73**, 255-267.
32. Y.Pan, Y.J.Li, H.Y.Zhao, J.M.Zheng, H.Xu, G.Wei, J.S.Hao, F.D.Cui, *Int. J. Pharm.* 2002, **249**, 139-147.
33. R.Bodmeier, H.G.Chen, O.Paeratakul, *Pharm. Res.* 1989, **6**, 413-417.
34. R.N.Wijesena, N.Tissera, Y.Y.Kannagara, Y.Lin, G.A.J.Amaratunga, K.M.N.De silva, *Carbohyd Polym.* 2015, **117**, 731-738.
35. Y.Wu, W.Yang, C.Wang, J.Hu, S.Fu, *Int J Pharm.* 2005, **295**, 235–245.
36. A.J.Bard, H.Lund, 1978. Marcel Decker. Inc. New York. vol. XII, 453–455.
37. R.G.Lima, P.S.Bonato, R.S.da Silva, *J. Pharm. Biomed. Anal.* 2003, **32**, 337-343.
38. H.Jung, L.Medina, L.Garcı´a, I.Fuentes, R.Moreno-Esparza, *J. Pharm.Pharmacol.* 1998, **50**, 43-48.

39. D.A.Skoog, F.T.Holler, T.A.Nieman, 1998. Principles of Insrumental Analysis. 5th ed. Harcourt Brace College Publisher, Florida. pp. 13-14.
40. H.De Ruyck, R.Van Renterghem, H.De Ridder, D.De Brabander, *Food Control*. 2000, **11**, 165-173.

Legend to Figures

Figure 1: Differential pulse voltammogram of (a) Extracting solvent [Acetic acid and methanol (1:4)], (b) Removed solution from electrode having acetic acid, methanol and ABZ and (c) Fresh solution of ABZ in extracting solvent [acetic acid and methanol (1:4)].

Figure 2: Schematic presentation for the preparation of electrochemical MIP sensor on gold electrode.

Figure 3: FTIR spectrum of chitosan nanoparticles.

Figure 4 : AFM image of chitosan nanoparticles [$Roughness_{rms}$ 2.89 nm, $Roughness_{av}$ 2.29; Grains 2173]

Figure 5: Cyclic voltammograms of the imprinted polymer films on gold electrode: potential cycling from -0.5 to1.5 V at a scan rate of 100mV/s for 30 cycles with 3mM/L ABZ, 0.2 % (w/v) chitosan nanoparticle and 0.5 M PBS as the supporting electrolyte, 20% glutaraldehyde as cross-linking agent. (a) MIP-coated imprinted film (b) non imprinted film (NIP)

Figure 6: DPV plots on bare gold electrode, MIP-coated electrode, NIP-coated electrode and adduct (ADD)-coated electrode in 0.10 M $K_3[Fe(CN)_6]$ solution.

Figure 7: Rebinding of ABZ molecules: DPV of ABZ solutions at MIP modified gold electrodes at various concentrations of ABZ in 0.10 M $K_3[Fe(CN)_6]$ solution.

Figure 8: DPV plots showing rebinding of ABZ molecules by MIP-coated electrode and NIP-coated electrode.

Figure 9: Comparative study on the rebinding of abz molecules by MIP and NIP at various concentrations of ABZ by (a) MIP-coated electrode (b) NIP-coated electrode.

Figure 10: Comparative study on the rebinding of ABZ molecules by MIP at varying pH.

Figure 11: Changes in MIP-coated gold electrode current in response to various structural analogues with ABZ in terms of their % recovery (5 ASA, Antipyrine, L-phenylalanine, 3 TAA)

Figure 12: Rebinding of ABZ molecules by MIP-coated electrodes with blood plasma at various concentrations of ABZ.

Figure 13: Calibration curve for rebinding of ABZ molecules by MIP-coated electrode at various concentrations of ABZ [R^2 0.9577, RSD 4.07%].

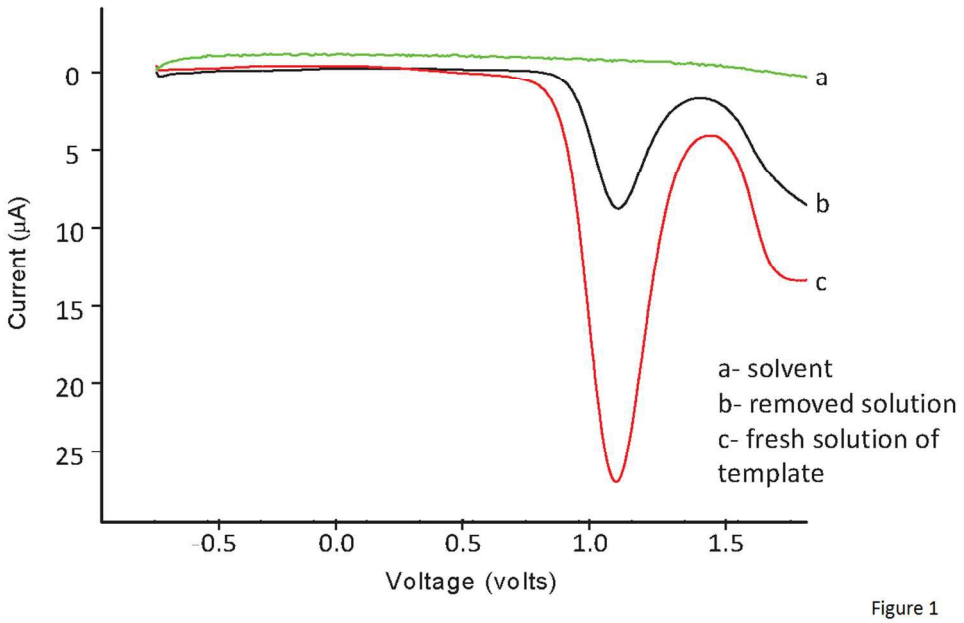

Figure 1

271x177mm (120 x 120 DPI)

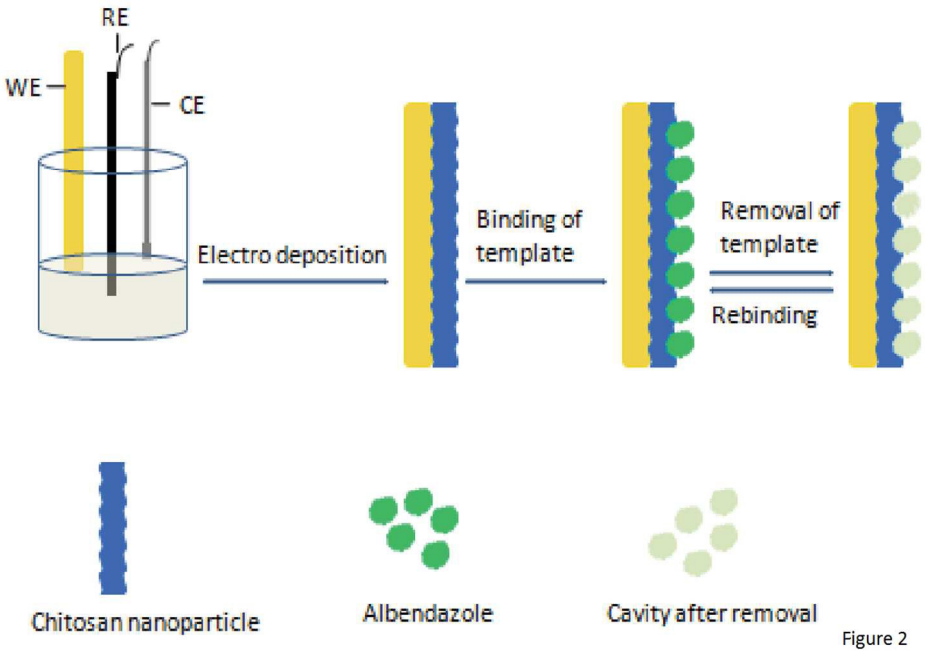

Figure 2

278x195mm (120 x 120 DPI)

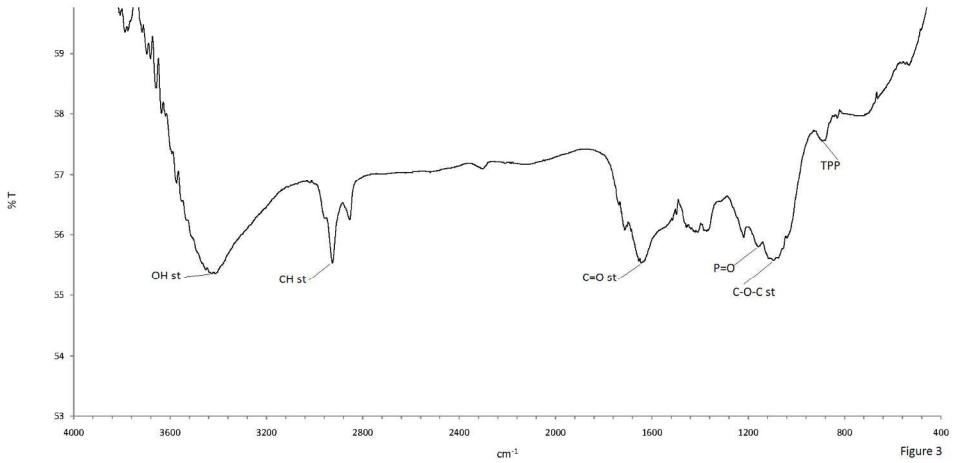

Figure 3

438x214mm (120 x 120 DPI)

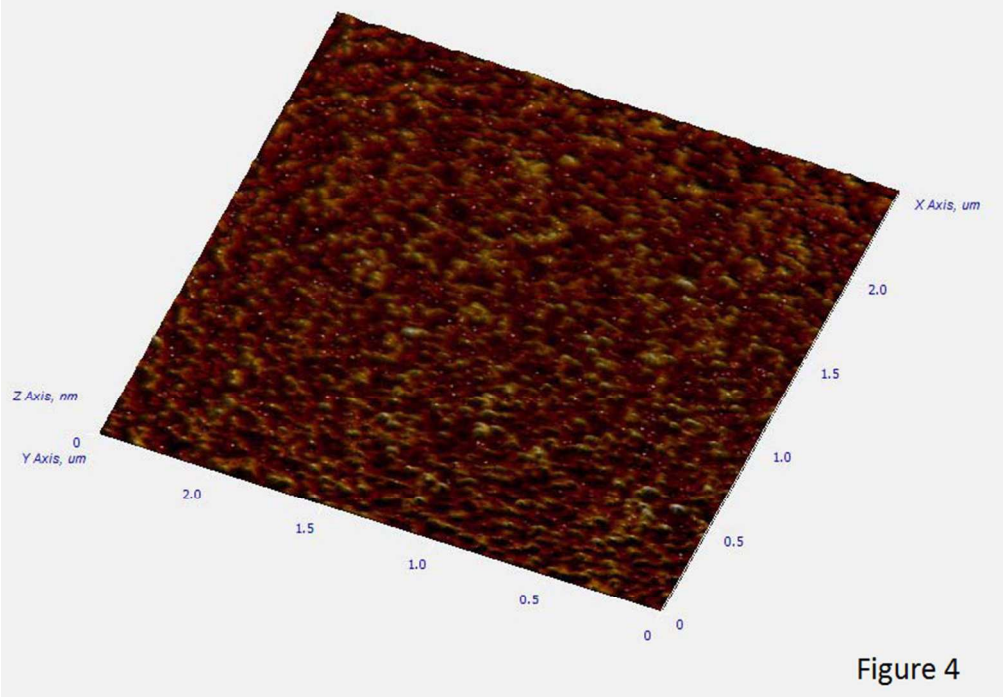

Figure 4

177x123mm (120 x 120 DPI)

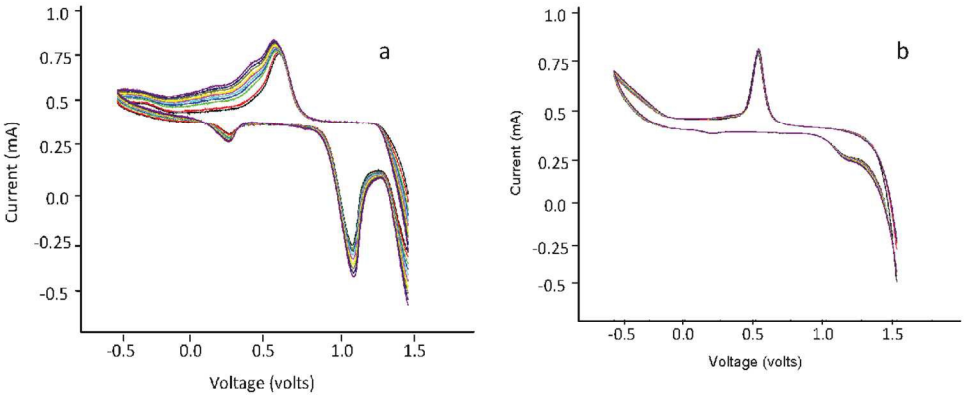

Figure 5

302x150mm (120 x 120 DPI)

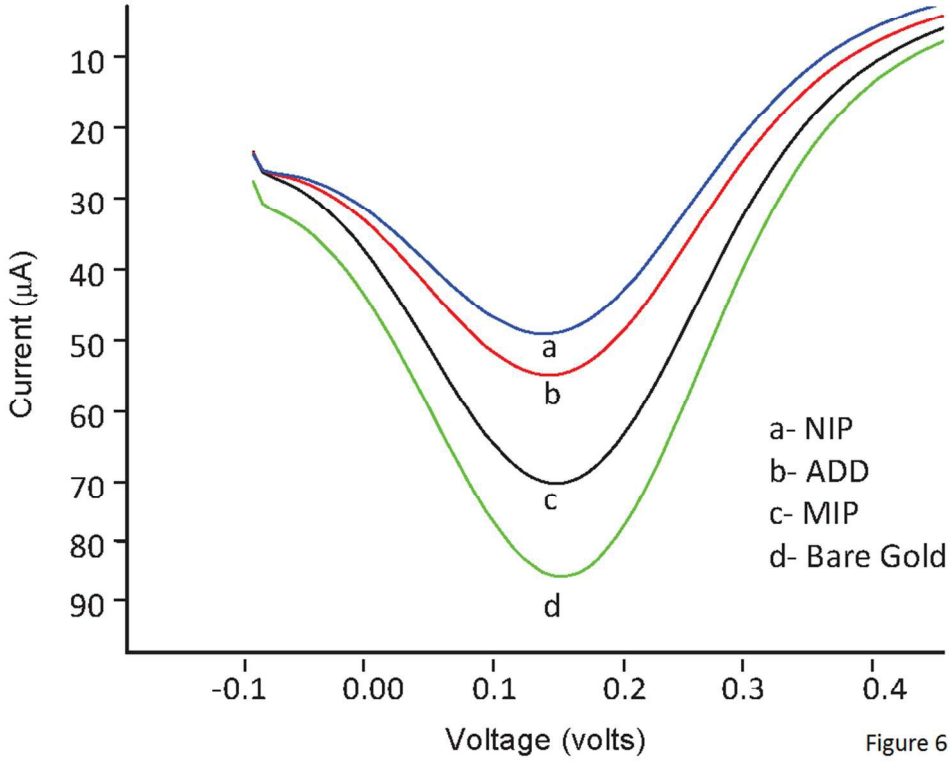

Figure 6

223x192mm (120 x 120 DPI)

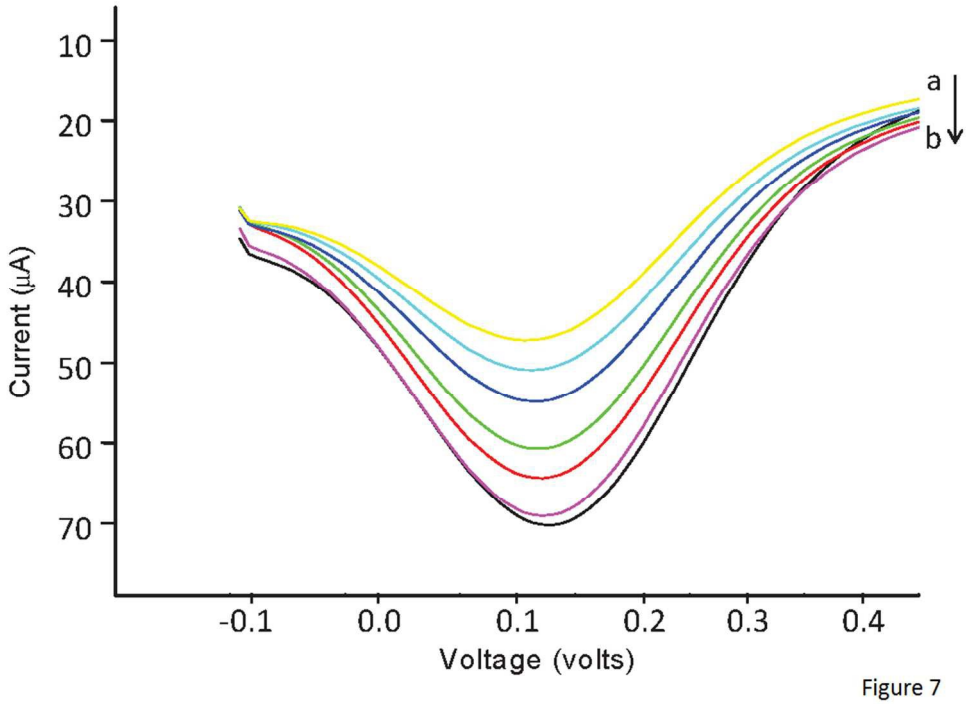

Figure 7

229x167mm (120 x 120 DPI)

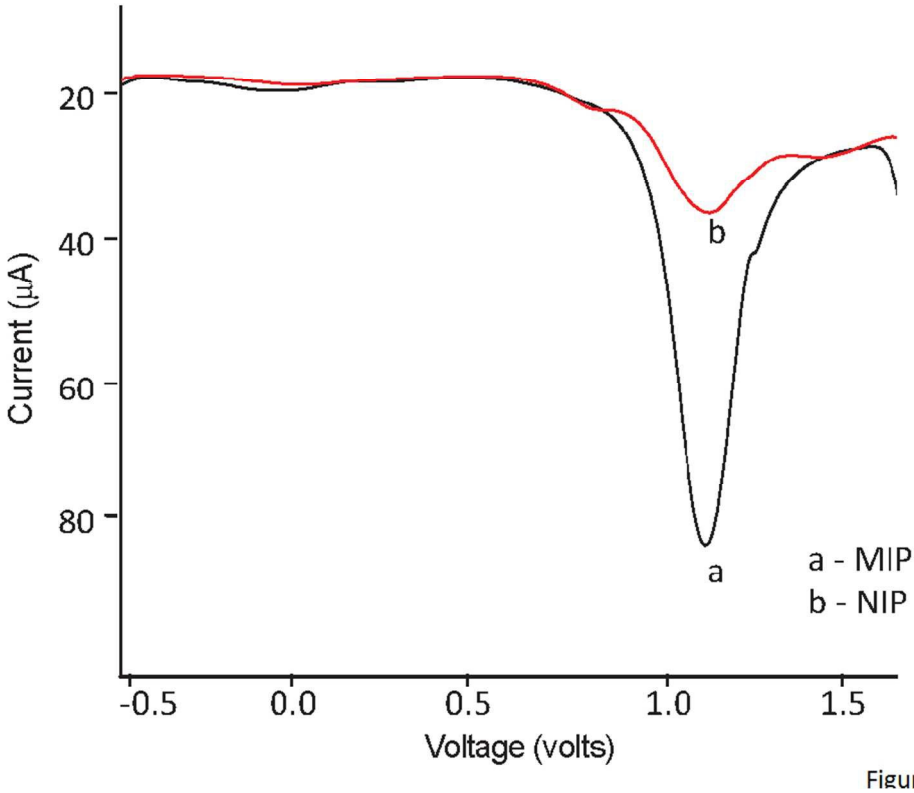

Figure 8

211x171mm (120 x 120 DPI)

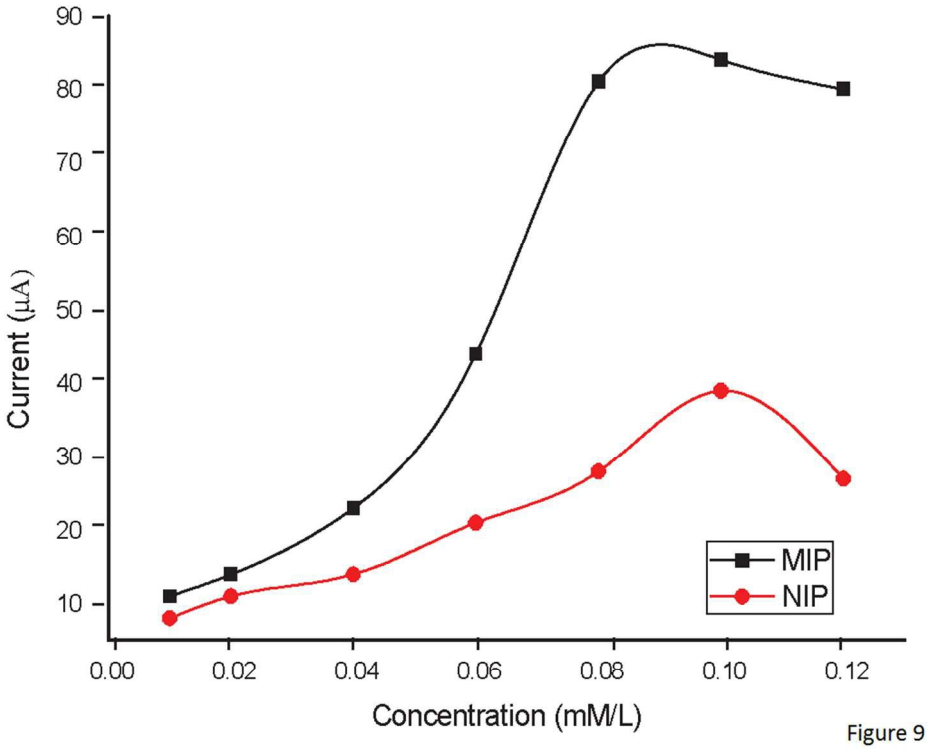

Figure 9

233x200mm (120 x 120 DPI)

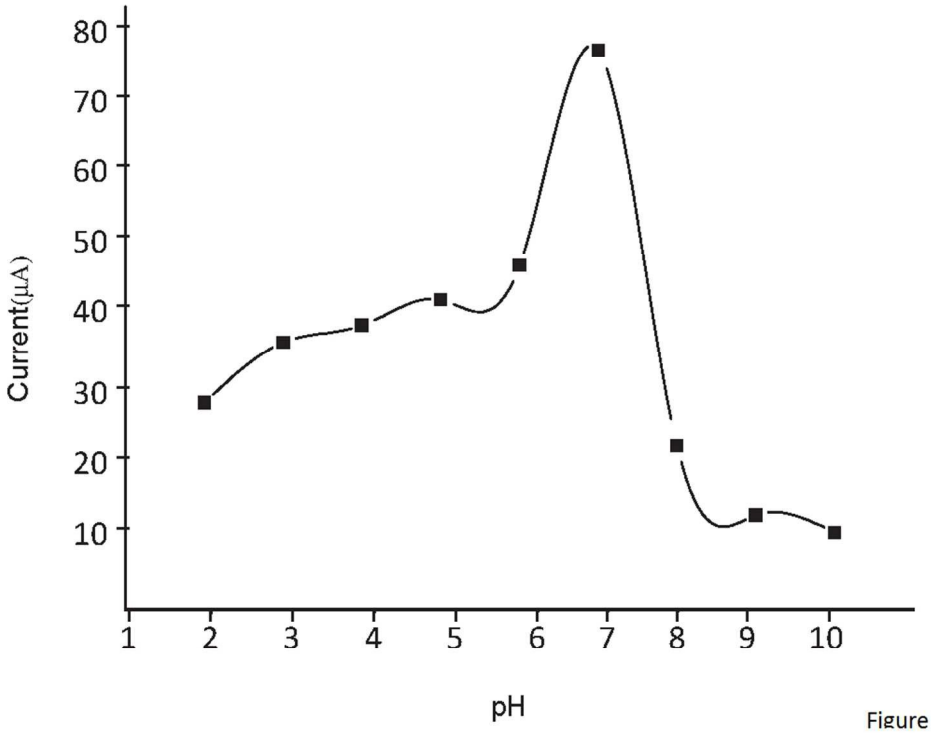

Figure 10

227x178mm (120 x 120 DPI)

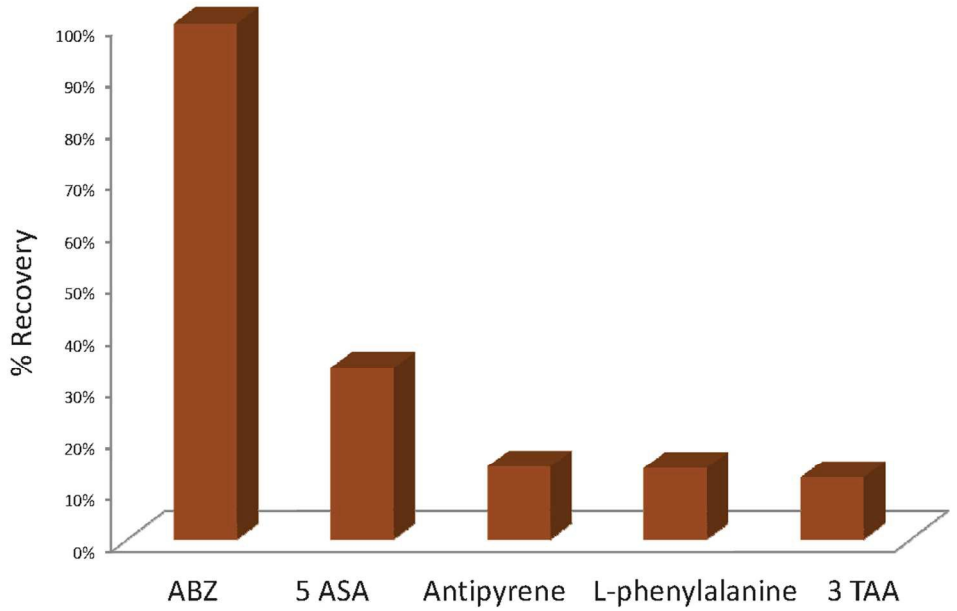

Figure 11

249x168mm (120 x 120 DPI)

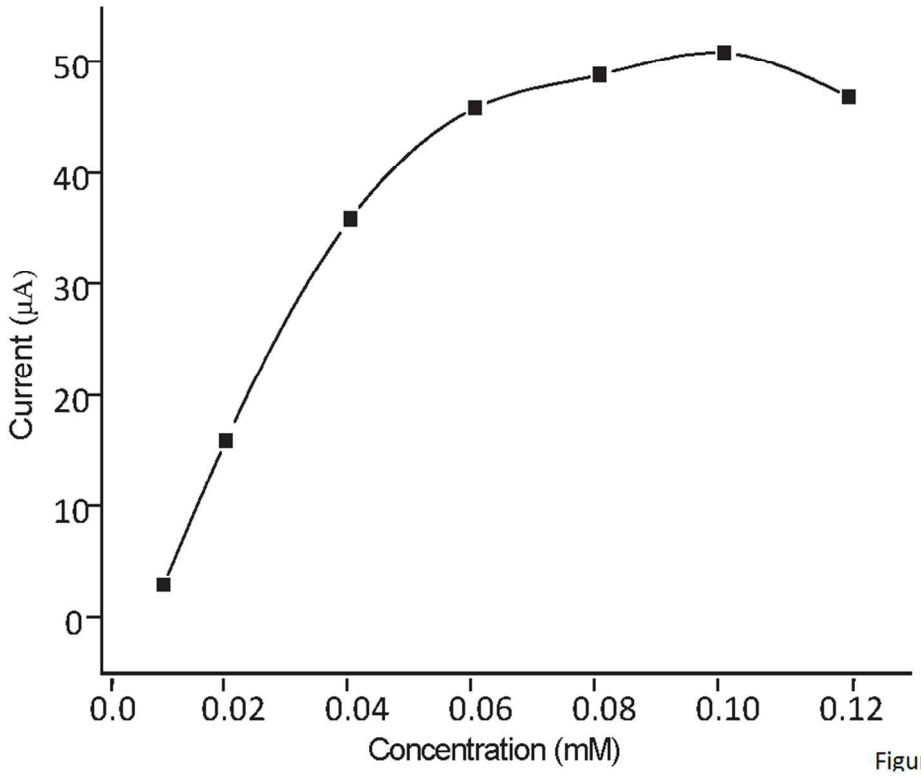

Figure 12

214x179mm (120 x 120 DPI)

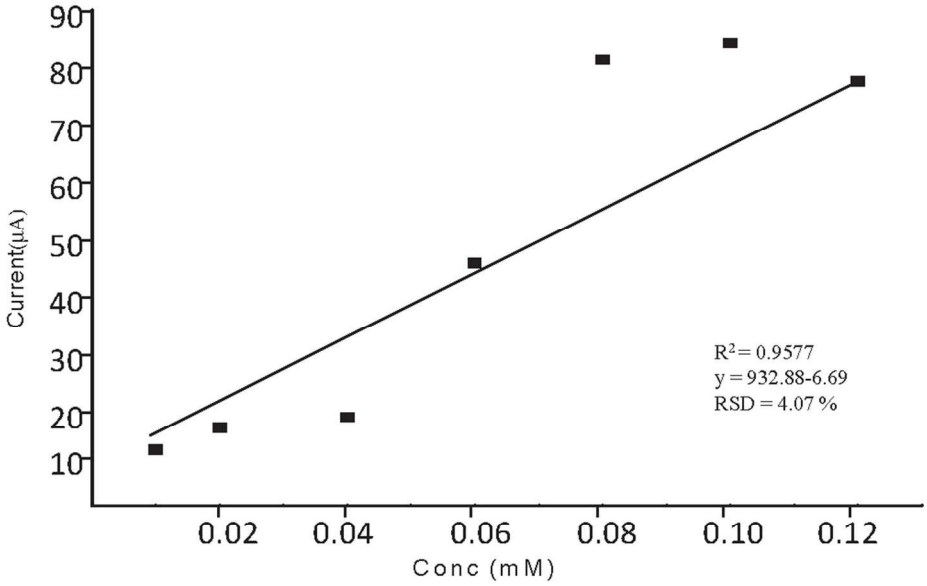

Figure 13

230x158mm (120 x 120 DPI)

Table 1: Comparison of different methods used for determination of ABZ

S. No.	Analytical method	LOD	References
1.	MISPE	0.012 µg L^{-1}	Ref 29
2.	Spectrophotometry	1.15 µg mL^{-1}	Ref 19
3.	DPV	0.106 µg mL^{-1}	Ref 8
4.	LSV	6.367 µg mL^{-1}	Ref 11
5.	SWV	0.164 µg mL^{-1}	Ref 8
6.	HPLC	0.02 µg mL^{-1}	Ref 17
7.	LC	0.006 µg mL^{-1}	Ref 14
8.	DPCSV	0.0027 µg mL^{-1}	Ref 9
9.	HPLC	0.0038 µg mL^{-1}	Ref 40
10.	LSV	7.959 µg mL^{-1}	Ref 8
11.	DPV	0.0166 µg mL^{-1}	Ref 12
12.	SWV	0.088 µg mL^{-1}	Ref 10
13.	HPLC	0.05 µg mL^{-1}	Ref 18
14	HPLC	0.06 µg mL^{-1}	Ref 16
15	Electrochemical MIP Sensor	0.119 µg mL^{-1}	This work

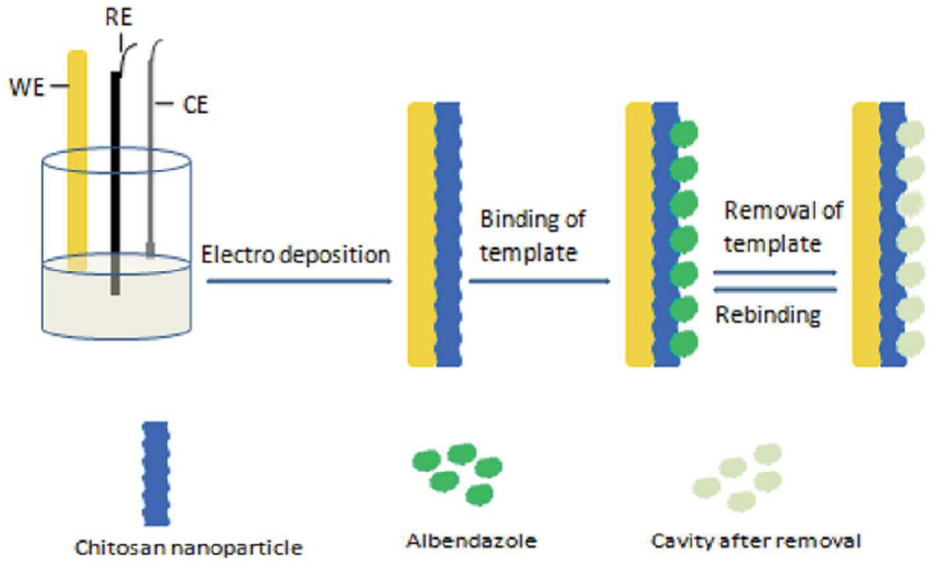

A biopolymeric nano-receptor for selective and sensitive recognition of albendazole

139x98mm (120 x 120 DPI)